

## KLOE / KLOE2

A. Antonelli, M. Antonelli, D. Babusci, G. Bencivenni, S. Bertolucci,  
C. Bloise (Resp. Naz.), F. Bossi, P. Campana, G. Capon, T. Capussela (Ass. Ric.),  
P. Ciambrone, E. De Lucia (Art. 23), P. de Simone, D. Domenici (Ass. Ric.),  
M. Dreucci (Art. 2222), G. Felici, C. Gatti, S. Giovannella, F. Happacher (Art. 23),  
M. Jacewicz (Bors. PD), J. Lee-Franzini (Ass.), M. Martini (Ass.), S. Miscetti,  
M. Moulson, S. Müeller (Art. 23), F. Murtas, M. Palutan, V. Patera (Ass.),  
P. Santangelo, B. Sciascia, A. Sciubba (Ass.), T. Spadaro,  
O. Vasquez Doce (Art. 23), G. Venanzoni, R. Versaci (Ass.)

Technical Staff:

M. Anelli, M. Carletti, G. Fortugno, M. Iannarelli, R. Rosellini, F. Sborzacchi, E. Turri

### 1 Outline

During 2008 the KLOE Collaboration has continued to work on data analysis and progressed on the plans and the preparatory work for data-taking in year 2009-2010 as well as on the R&D activities for further detector upgrades.

On the Kaon sector, big efforts have been devoted to the analysis of the  $K_{e2}$  channel. The ratio  $BR(K_{e2})/BR(K_{\mu2})$  is sensitive to couplings beyond the Standard Model (SM)<sup>1)</sup> that should enhance the elicity-suppressed  $K_{e2}$  mode well above SM prediction. In order to select the largest possible sample of  $K_{e2}$  decays, a completely new set of procedures, for the identification of the signal and the control samples, for the comparison and the correction of Monte Carlo data, for the evaluation of the systematics, has been devised and carefully studied. This is discussed in Sect. 2.1.

The KLOE results on  $|V_{us}|$ , obtained thanks to many, consistent, precision measurements summarized in Sect. 2.2, have been selected as one of the best achievements of year 2008, and presented to the INFN “Comitato di Valutazione”, on July, 9.

Sect. 2.3 is devoted to the study of the quantum coherence of neutral Kaon pairs in the final state  $\pi^+\pi^-\pi^+\pi^-$ . Other branching ratio measurements, of the  $K_S \rightarrow e^+e^-$ , and the  $K^\pm \rightarrow \pi^\pm\pi^+\pi^-$ , are described in Sect. 2.4 and 2.5 respectively.

For the hadronic cross section, the analysis of  $\pi\pi\gamma$  events with photons emitted at low polar angle ( $|\cos(\theta)| > \cos(\pi/12)$ ), using Bhabha events as normalization, has been completed and published on PLB 672(2009)285. Independent results on the same topic are provided by the normalization of the  $\pi\pi\gamma$  sample to the  $\mu\mu\gamma$  events, by the study of the  $\pi\pi\gamma$  final state with reconstructed photons at large angle, and by the analysis of off-peak data, taken at  $\sqrt{s} = 1$  GeV. A status report is presented in Sect. 3.1.

For the  $\eta$  decays, the measurement of the  $BR(\eta \rightarrow \pi\pi e e)$  at the 4% precision level has been finalized, as described in Sect. 3.2, and work is in progress on the radiative  $\pi\pi\gamma$  channel, reported in Sect. 3.3.

In June 2008 the plan for a new KLOE data taking, KLOE2, has been approved and funded. Test and revision of all the apparatus subsystems has started and the upgrade of the obsolete or inadequate components, including level-2 CPUs, online farm, data storage and the related software,

has planned and realized to a great extent.

A tagger for  $\gamma\gamma$  physics is being designed to be installed for the new data taking. The experimental setup consists of two stations to detect low, (160-230) MeV, and high, (435-490) MeV, energy electrons respectively. The first is located inside the KLOE detector,  $\sim 1$  m from the interaction region (IP), the second at the exit of the bending dipoles,  $\sim 11$  m from the IP. A report on the status of the project is given in Sect. 4.1.

R&D activities on the calorimeters to instrument the zone of the DAΦNE quadrupoles in the new interaction region are progressing and the realization of an entire module (1/12 of the whole azimuthal acceptance),  $\sim 90$  cm long, constituted by scintillating tiles and optically coupled fibers for signal transmission, as described in Sect. 4.2, is planned by the end of 2009.

Finally, Sect. 4.3 reports about the design and the test results on a prototype of the cylindrical triple-GEM chamber which is being studied for the KLOE tracking upgrade as a new inner tracker detector to be installed close to the beam pipe at the interaction region.

## 2 Results in kaon physics

### 2.1 SM test with $K_{e2}^{\pm}$ decays

Recently it has been pointed out that, in a SUSY framework, sizeable violations of lepton universality can be expected in  $K_{l2}$  decays <sup>1)</sup> from the couplings to a charged Higgs boson  $H^+$ . In a scenario which allows for violation of lepton flavor, the value of the ratio  $R_K = \Gamma(K \rightarrow e\nu)/\Gamma(K \rightarrow \mu\nu)$ , which in the SM is precisely determined, would be modified to:

$$R_K^{LFV} = R_K^{SM} \left[ 1 + \left( \frac{m_K^4}{m_{H^\pm}^4} \right) \left( \frac{m_\tau^2}{m_e^2} \right) |\Delta_{13}|^2 \tan^6 \beta \right]. \quad (1)$$

With the lepton flavor violating term  $\Delta_{13}$  of the order of  $10^{-4} - 10^{-3}$ , as expected from neutrino mixing, and moderately large values of  $\tan\beta$  and  $m_{H^\pm}$ , SUSY contributions may enhance  $R_K$  up to a few percent. A measurement of the  $K^\pm \rightarrow e^\pm\nu$  decay,  $K_{e2}$ , at the per cent accuracy is challenging, since one has to face a signal to background ratio which is of the same order of magnitude of  $R_K$ . High background rejection has then to be achieved while keeping at the same time a good control of systematics.

For this measurement we decided to perform a “direct search” for  $K_{e2}$  and  $K_{\mu2}$  decays without tagging, to keep the statistical uncertainty on the number of counts below 1%. The presence of a one-prong decay vertex in the drift chamber volume with a secondary charged decay track with relatively high momentum (180 ÷ 270 MeV) is required. A very good separation between  $K_{e2}$  events and the background, which is dominated by  $K_{\mu2}$ , is obtained by using the lepton mass squared,  $M_{lep}^2$ , evaluated from the momenta of the kaon and the charged decay particle, assuming zero neutrino mass. Further background rejection comes by combining all of the calorimeter informations into a PID discriminating variable ( $NNPid$  in the following).

The number of signal events is extracted from a likelihood fit to the two-dimensional  $M_{lep}^2 - NNPid$  distribution, using MC shapes for signal and background. The number of signal events obtained from the fit is  $N_{e2} \sim 13\,800 \pm 140$ ; the projection of the fit result on the  $M_{lep}^2$  axis for positive kaons is compared to data in fig.1. The number of  $K_{\mu2}$  events in the same data set is

extracted from a similar fit to the  $M_{\text{lep}}^2$  distribution, where no PID information is used. Using the number of observed  $K_{e2}$  and  $K_{\mu2}$  events, we get as a final result

$$R_K = (2.493 \pm 0.025 \pm 0.019) \times 10^{-5}, \quad (2)$$

with 1.3% total error. This value is compatible within errors with the SM prediction,  $R_K^{SM} = (2.472 \pm 0.001) \times 10^{-5}$ . Figure 2 shows the strong constraints on  $\tan\beta$  and  $m_{H^\pm}$  given by the KLOE  $R_K$  result. For a moderate value of  $\Delta_{13} \approx 5 \times 10^{-4}$ , the region  $\tan\beta > 50$  is excluded for charged Higgs masses up to 1000 GeV/ $c^2$  at 95% CL.

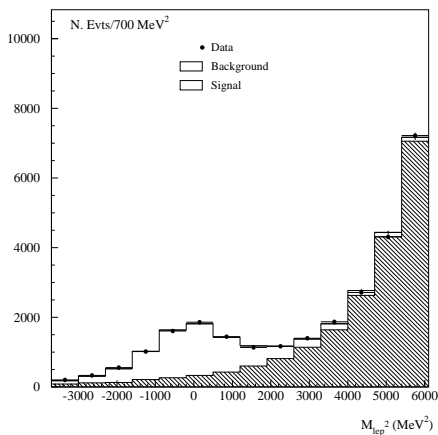


Figure 1: *Distribution of the squared lepton mass of the charged secondary track  $M_{\text{lep}}^2$ : filled dots are data, open dots the result from the maximum-likelihood fit.*

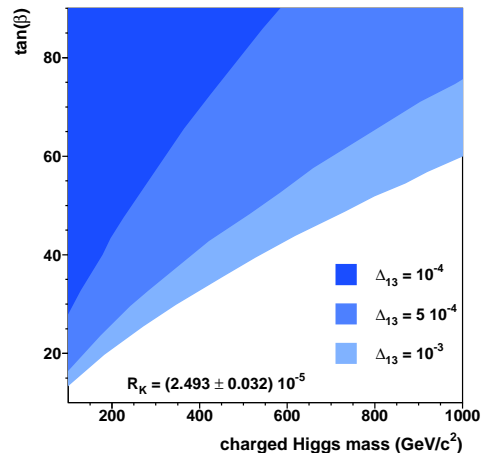


Figure 2: *Exclusion limits at 95% CL on  $\tan\beta$  and the charged Higgs mass  $m_{H^\pm}$  from  $R_K$  for different values of  $\Delta_{13}$ .*

## 2.2 $V_{us}$ and lepton universality with kaons

During the last years, we measured most of the decay branching ratios of  $K_S$  and  $K_L$  <sup>2) 3)</sup>. We published this year new measurements of  $K^\pm$  semileptonic decay branching ratios <sup>4)</sup> and of the  $K^\pm$  two-body decay branching ratio,  $\text{BR}(K^+ \rightarrow \pi^+\pi^0)$  <sup>5)</sup>, having published already in 2006 the  $\text{BR}(K^+ \rightarrow \mu\nu)$  <sup>6)</sup>. We have also measured the  $K_L$  lifetime <sup>7)</sup> and we recently published a new measurement of the  $K^\pm$  lifetime. Finally, the shape of the form factors in semileptonic decays have been measured for both  $K_{e3}$  <sup>8)</sup> and  $K_{\mu3}$  decays <sup>9)</sup>. The above results provide the basis for the determination of the CKM parameter  $V_{us}$ , and a test of the unitarity of the quark flavor matrix. We also test the lepton universality in  $K_{l3}$  decays and place bounds on new physics using measurements of  $V_{us}$  from  $K_{l2}$  and  $K_{l3}$  decays. A well organized compendium of all of our data has been recently published, and presented in summer 2008 to the International Advisory Committee of the INFN as one of the major experimental results achieved during the year. We summarize here the main results.

Using our determinations of the kaon semileptonic decay rates, we obtained the values of  $f_+(0)V_{us}$  for  $K_{Le3}$ ,  $K_{L\mu3}$ ,  $K_{Se3}$ ,  $K_{e3}^\pm$ , and  $K_{\mu3}^\pm$  decay modes. It is worth noting that the only

external experimental input to this analysis is the  $K_S$  lifetime. The five different determinations have been averaged, taking into account all known correlations. We find

$$f_+(0) V_{us} = 0.2157 \pm 0.0006, \quad (3)$$

with  $\chi^2/\text{ndf} = 7.0/4(13\%)$ .

Comparison of the values of  $f_+(0) V_{us}$  for  $K_{e3}$  and  $K_{\mu 3}$  modes provides a test of lepton universality. Specifically,

$$r_{\mu e} = \frac{(f_+(0) V_{us})_{\mu 3, \text{exp}}^2}{(f_+(0) V_{us})_{e 3, \text{exp}}^2} = \frac{\Gamma_{\mu 3}}{\Gamma_{e 3}} \frac{I_{e 3}(1 + \delta_{K e})^2}{I_{\mu 3}(1 + \delta_{K \mu})^2}, \quad (4)$$

where  $\delta_{K l}$  is a correction due to  $SU(2)$  breaking and photon radiation. The ratio  $r_{\mu e}$  is equal to the ratio  $g_\mu^2/g_e^2$ , with  $g_l$  the coupling strength at the  $W \rightarrow \ell \nu$  vertex. In the SM,  $r_{\mu e} = 1$ . Averaging between charged and neutral modes, we find

$$r_{\mu e} = 1.000 \pm 0.008. \quad (5)$$

This has to be compared with the sensitivity obtained in  $\pi \rightarrow \ell \nu$  decays,  $(r_{\mu e})_\pi = 1.0042(33)$ , and in  $\tau$  leptonic decays,  $(r_{\mu e})_\tau = 1.000(4)$  <sup>10)</sup>.

Lattice evaluations of  $f_+(0)$  are rapidly improving in precision. For example, the RBC and UKQCD Collaborations have recently obtained  $f_+(0) = 0.9644(49)$  from a lattice calculation with  $2 + 1$  flavors of dynamical domain-wall fermions <sup>11)</sup>. Using their value of  $f_+(0)$ , with our determination of  $f_+(0) V_{us}$ , with 2.8 per mill fractional accuracy, we obtain  $V_{us} = 0.2237(13)$ .

The availability of precise lattice evaluations for the pion- and kaon-decay constants  $f_\pi$  and  $f_K$  allows to use the relation between  $\Gamma(K_{\mu 2})/\Gamma(\pi_{\mu 2})$  and  $|V_{us}|^2 / |V_{ud}|^2$ , with the advantage that lattice-scale uncertainties and radiative corrections largely cancel out in the ratio <sup>12)</sup>. From our measurements of  $\text{BR}(K_{\mu 2})$  and  $\tau_\pm$ , and using  $\Gamma(\pi_{\mu 2})$  from <sup>10)</sup>, we evaluate:

$$V_{us}/V_{ud} \times f_K/f_\pi = 0.2766 \pm 0.0009. \quad (6)$$

Using the recent lattice determination of  $f_K/f_\pi$  from the HPQCD/UKQCD collaboration,  $f_K/f_\pi = 1.189(7)$  <sup>13)</sup>, we finally obtain  $V_{us}/V_{ud} = 0.2326 \pm 0.0015$ .

To test the unitarity of the quark mixing matrix, we combine all the information from our measurements on  $K_{\mu 2}$ ,  $K_{e 3}$ ,  $K_{\mu 3}$ , together with superallowed  $0^+ \rightarrow 0^+$  nuclear  $\beta$  decays (fig.3). The best estimate of  $|V_{us}|^2$  and  $|V_{ud}|^2$  can be obtained from a fit to our results  $V_{us} = 0.2237(13)$  and  $V_{us}/V_{ud} = 0.2326(15)$ , together with  $V_{ud} = 0.97418(26)$  <sup>14)</sup>. The fit gives  $|V_{us}|^2 = 0.0506(4)$  and  $|V_{ud}|^2 = 0.9490(5)$ , with  $\chi^2/\text{ndf} = 2.34/1$  (13%) and a correlation coefficient of 3%. The values obtained confirm the unitarity of the CKM quark mixing matrix as applied to the first row. We find:

$$|V_{us}|^2 + |V_{ud}|^2 - 1 = -0.0004 \pm 0.0007 \quad (\sim 0.6\sigma). \quad (7)$$

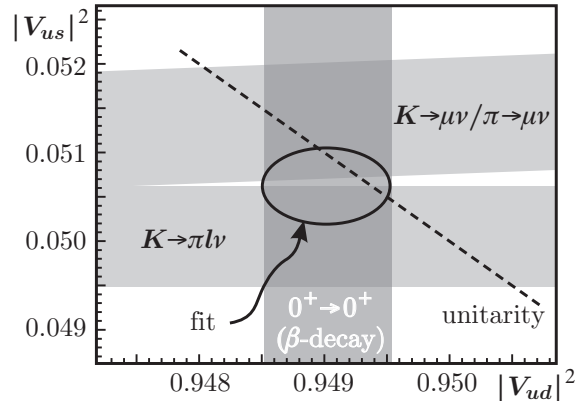


Figure 3: *KLOE* results for  $|V_{us}|^2$  and  $|V_{us}/V_{ud}|^2$ , together with  $|V_{ud}|^2$  from  $\beta$ -decay measurements. The ellipse is the  $1\sigma$  contour from the fit. The unitarity constraint is illustrated by the dashed line.

### 2.3 Quantum interferometry

The neutral kaon pair from  $\phi \rightarrow K^0 \bar{K}^0$  are produced in a pure quantum state with  $J^{PC} = 1^{--}$ . The decay intensity to any two possible final states  $f_1(t_1)$  and  $f_2(t_2)$ , integrated over all  $t_1$  and  $t_2$  for fixed  $\Delta t = t_1 - t_2$ , is expressed as:

$$I_{f_1, f_2}(\Delta t) = \frac{1}{2\Gamma} |\langle f_1 | K_S \rangle \langle f_2 | K_S \rangle|^2 \times \left[ |\eta_1|^2 e^{-\Gamma_L \Delta t} + |\eta_2|^2 e^{-\Gamma_S \Delta t} - 2(1 - \zeta) |\eta_1| |\eta_2| e^{-(\Gamma_L + \Gamma_S) \Delta t / 2} \cos(\Delta m \Delta t + \phi_2 - \phi_1) \right], \quad (8)$$

where  $\Delta t > 0$ , and  $\Gamma \equiv \Gamma_L + \Gamma_S$ . The last term is due to interference between the decays to states  $f_1$  and  $f_2$  and  $\zeta=0$  in quantum mechanics. Fits to the  $\Delta t$  distribution provide measurements of the magnitudes and phases of the parameters  $\eta_i = \langle f_i | K_L \rangle / \langle f_i | K_S \rangle$ , as well as of the  $K_L$ - $K_S$  mass difference  $\Delta m$  and the decay widths  $\Gamma_L$  and  $\Gamma_S$ .

Such fits also allow to test fundamental properties of quantum mechanics. For example, quantum-mechanical coherence can be tested by choosing  $f_1 = f_2$ . In this case, because of the antisymmetry of the initial state and the symmetry of the final state, there should be no events with  $\Delta t = 0$ . The analysis of the  $\Delta t$  distribution for  $K_S K_L \rightarrow \pi^+ \pi^- \pi^+ \pi^-$  events on a statistics of  $\sim 1500 \text{ pb}^{-1}$  of data integrated during year 2004-2005 has been recently completed. The  $\Delta t$  distribution is fit with a function of the form of eq.8, including the experimental resolution and the peak from  $K_L \rightarrow K_S$  regeneration in the beam pipe. Observation of  $\zeta \neq 0$  would imply loss of quantum coherence. The value of  $\zeta$  depends on the basis,  $K^0 - \bar{K}^0$  or  $K_S - K_L$  used in the analysis. Using the  $K^0 - \bar{K}^0$  basis we find

$$\zeta = (1.4 \pm 9.5_{\text{stat}} \pm 3.8_{\text{syst}}) \times 10^{-7} \quad (9)$$

which improves by a factor of two with respect to the KLOE result published in 2006<sup>15)</sup>, based on  $\sim 400 \text{ pb}^{-1}$  of data.

In the context of quantum gravity, *CPT* violation effects might occur in correlated neutral kaon states<sup>16, 17)</sup>, where the resulting loss of particle-antiparticle identity could induce a

breakdown of state correlation imposed by Bose statistics. As a result, the initial state can be parametrized as:

$$\begin{aligned}
|i\rangle &= \frac{1}{\sqrt{2}} (|K^0, \vec{p}\rangle |\bar{K}^0, -\vec{p}\rangle - |\bar{K}^0, \vec{p}\rangle |K^0, -\vec{p}\rangle) \\
&+ \frac{\omega}{\sqrt{2}} (|K^0, \vec{p}\rangle |\bar{K}^0, -\vec{p}\rangle + |\bar{K}^0, \vec{p}\rangle |K^0, -\vec{p}\rangle) ,
\end{aligned} \tag{10}$$

where  $\omega$  is a complex parameter describing a completely novel  $CPT$  violation phenomenon, not included in previous analyses. Its order of magnitude could be at most  $|\omega| \sim [(m_K^2/m_{\text{Planck}})/\Delta\Gamma]^{1/2} \sim 10^{-3}$  with  $\Delta\Gamma = \Gamma_S - \Gamma_L$ . Inserting the modified initial state in the expression of the  $K_S K_L \rightarrow \pi^+ \pi^- \pi^+ \pi^-$  decay intensity, and fitting the  $\Delta t$  distribution as in the case of the previous analysis, we obtain the following results for the real and imaginary parts of  $\omega$ :

$$\text{Re}(\omega) = (-1.6_{-2.1}^{+3.0} \pm 0.4) \times 10^{-4}, \quad \text{Im}(\omega) = (-1.7_{-3.0}^{+3.3} \pm 1.2) \times 10^{-4}. \tag{11}$$

This can be translated into an upper limit on the absolute value,  $|\omega| < 1.0 \times 10^{-3}$  at 95% CL, thus reaching the interesting Planck's scale region. Also in this case, the analysis of the full data sample allowed to improve by a factor of two with respect to the published results <sup>15)</sup>.

#### 2.4 Direct search of $K_S \rightarrow e^+ e^-$

This decay is a flavour-changing neutral current process, suppressed in the SM, with an amplitude dominated by the two photon intermediate state. Using ChPT to  $\mathcal{O}(p^4)$ , one obtains the prediction  $\text{BR}(K_S \rightarrow e^+ e^-) \sim 2 \times 10^{-14}$  <sup>18)</sup>. A value significantly higher could indicate new physics. Prior to KLOE, the best experimental limit on this decay was set by CPLEAR,  $\text{BR}(K_S \rightarrow e^+ e^-) \leq 1.4 \times 10^{-7}$  at 90% CL <sup>19)</sup>.

We performed a search for the  $K_S \rightarrow e^+ e^-$  decay using  $1.9 \text{ fb}^{-1}$  of integrated luminosity. A MC background sample of comparable statistics and a large MC signal sample have been also used in the analysis. After K-crash tag, we search for the signal by requiring two tracks of opposite charge originating near the IP. The two tracks are required to have an invariant mass  $M_{ee}$ , evaluated in the electron hypothesis, in a  $\sim 20$  MeV window around the nominal  $K_S$  mass. This cut is particularly effective on  $K_S \rightarrow \pi^+ \pi^-$  events, which peak at  $M_{ee} \sim 409$  MeV. After it the background is dominated by  $K_S \rightarrow \pi^+ \pi^-$  with at least one pion wrongly reconstructed, and by  $\phi \rightarrow \pi^+ \pi^- \pi^0$  events. The  $K_S$  events are strongly reduced by cutting on the track momentum in the  $K_S$  rest frame, which is expected to be  $\sim 206$  MeV for  $K_S \rightarrow \pi^+ \pi^-$  decays. To reject  $\phi \rightarrow \pi^+ \pi^- \pi^0$  events we use instead  $|\vec{p}_{\text{miss}}| = |\vec{p}_\phi - \vec{p}_{K_S} - \vec{p}_{K_L}|$ , where  $K_S$  and  $K_L$  momenta are evaluated from the charged tracks and from the K-crash tag, respectively. The value of  $|\vec{p}_{\text{miss}}|$  peaks at zero for the signal, within the experimental resolution of few MeV. It spreads towards higher values for  $\phi \rightarrow \pi^+ \pi^- \pi^0$  events. The residual background, both from  $K_S \rightarrow \pi^+ \pi^-$  and  $\phi \rightarrow \pi^+ \pi^- \pi^0$  decays, is rejected identifying the two electrons by ToF, and by using the properties of the associated calorimetric cluster. The reliability of the MC background simulation is checked after each step of the selection on the invariant mass sidebands. At the end of the analysis chain, we don't count any event in the signal box; the background estimate is also compatible with zero. The upper limit on the number of signal events is therefore  $N_{ee} = 2.3$  at 90% CL. The signal selection efficiency, after tagging, is  $\sim 47\%$ . Such performance in terms of exceptional background rejection ( $> 10^8$ )

with an acceptable signal efficiency, has been achieved largely thanks to the very good momentum resolution of our DC. To obtain an upper limit for the  $BR(K_S \rightarrow e^+e^-)$ , we normalize  $N_{ee}$  to the  $K_S \rightarrow \pi^+\pi^-$  decays observed in the same data sample. Finally, we obtain:

$$BR(K_S \rightarrow e^+e^-) \leq 9 \times 10^{-9} \quad \text{at 90\% CL}, \quad (12)$$

which represents a factor of  $\sim 15$  improvement with respect to the best previous limit. This result, submitted for publication at the end of 2008, has been recently published by Phys. Lett. B <sup>20</sup>.

## 2.5 Measurement of $BR(K^\pm \rightarrow \pi^\pm\pi^+\pi^-)$

The measurement of the BR of this decay completes the KLOE program of precise and fully inclusive kaon dominant BR's measurements. The most recent result,  $BR(K^\pm \rightarrow \pi^\pm\pi^+\pi^-) = (5.56 \pm 0.20)\%$  <sup>21</sup>, dates back to more than 30 years ago.

We plan to use two normalization samples given by the two tags,  $K_{\mu 2}$  and  $K_{\pi 2}$ . The track of the tagged kaon is backward extrapolated to the interaction point, then the kinematic of the decay  $\phi \rightarrow K^+K^-$  allows to define the path of the signal kaon (direction and momentum).

The decay products of the kaons have low momentum, less than 200 MeV/c, and curl up in the KLOE magnetic field (0.52 T); this increases the probability to reconstruct broken tracks and fake vertices. Selecting kaon decays before the inner wall of the drift chamber, the maximum number of tracks to be reconstructed is three instead of four, and the quality of the reconstruction improves.

We require at least two reconstructed tracks in the DC (pion candidates), and if their backward extrapolations give a vertex on the path of the signal kaon we evaluate the missing mass of the decay. Work is in progress to finalize the evaluation of the efficiency, and the associated systematic error, of the reconstruction procedure described above, using MC samples corrected to take into account tiny data-MC discrepancies in tracking.

Figure 4 shows the comparison between data and MC missing mass spectrum, that peaks in the pion mass region. Figure 5 shows the contributions to the MC missing mass distribution due to the signal selected sample and to the background; the ratio is  $S/B \simeq 18.6$ .

The good agreement between data and MC allows to perform event counting on the missing mass distribution with negligible systematic uncertainty.

## 3 Results in hadronic physics

### 3.1 The measurement of the hadronic cross section

During 2008, the analysis of the hadronic cross section measurement for the process  $e^+e^- \rightarrow \pi^+\pi^-$  from KLOE data taken in year 2002 has been finalized <sup>22</sup>. The dipion contribution to the muon anomaly,  $a_\mu^{\pi\pi}$ , in the interval  $0.592 < M_{\pi\pi} < 0.975$  GeV, has been measured with negligible statistical error and a 0.6% experimental systematic uncertainty. Radiative corrections increase the systematic uncertainty to 0.9%. Combining all errors we found:

$$a_\mu^{\pi\pi}(0.592 < M_{\pi\pi} < 0.975 \text{ GeV}) = (387.2 \pm 3.3) \times 10^{-10}.$$

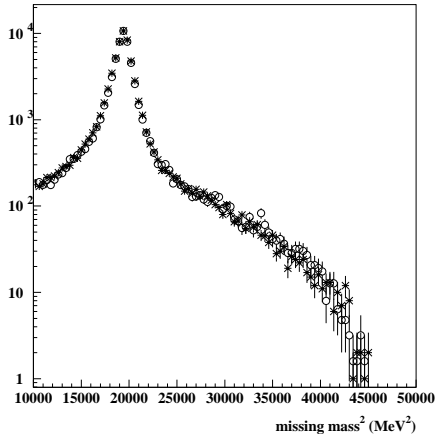


Figure 4:  $K\pi\pi$  missing mass distribution: empty dots are data, stars MC.

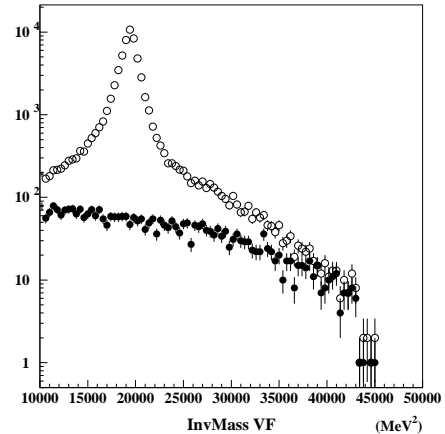


Figure 5: MC  $K\pi\pi$  missing mass distribution (empty dots), the background contribution is superimposed (filled dots).

This result represents an improvement of 30% on the systematic error with respect to our previous published value<sup>23)</sup>, and confirms the current disagreement between the standard model prediction for  $a_\mu$  and the measured value, as shown in fig. 6, left. The spectrum of the pion form factor is also in very good agreement with recent results from SND and CMD2 experiments at Novosibirsk<sup>24)</sup>, as shown in fig. 6, right.

Independent analyses are in progress:

- to measure  $\sigma_{\pi\pi(\gamma)}$  using detected photons emitted at large angle, improving knowledge of the FSR interference effects (in particular the  $f_0(980)$  contribution);
- to measure the pion form factor directly from the ratio, bin-by-bin, of  $\pi^+\pi^-\gamma$  to  $\mu^+\mu^-\gamma$  spectra;
- to extract the pion form factor from data taken at  $\sqrt{s} = 1$  GeV, off the  $\phi$  resonance, where  $\pi^+\pi^-\pi^0$  background is negligible.

We organized the PHIPSI08-Workshop at the Frascati laboratory, in April 2008, bringing together more than 120 physicists<sup>27)</sup>. In this workshop our final result on dipion contribution to the muon anomaly was presented.

In addition, a meeting of the Working Group on Radiative Corrections and MC Generators for Low Energies, was held on April 10 at the LNF, with theorists and experimentalists discussing current status and developments on the calculations of radiative corrections and Monte Carlo generators for physics in the continuum at low energy.

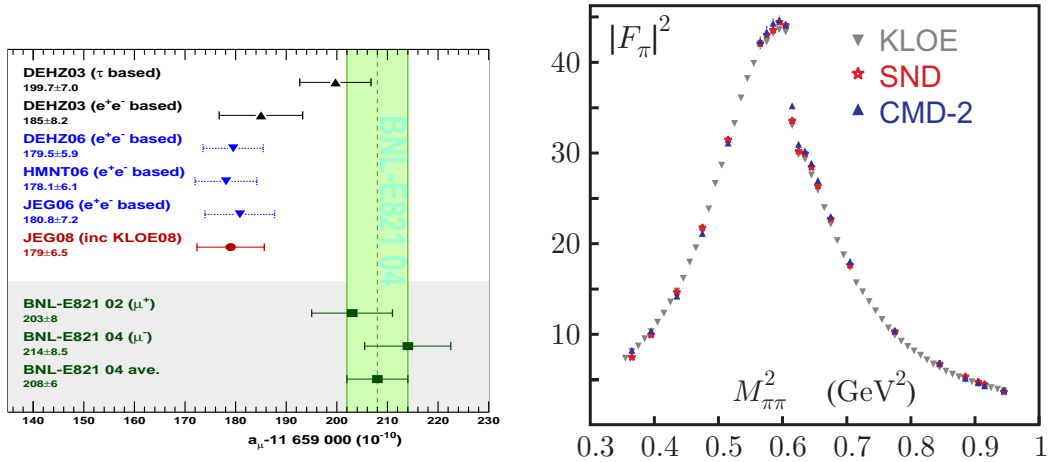


Figure 6: *Left: Comparison of the theoretical prediction for  $a_\mu$  <sup>25)</sup> with the BNL measurement <sup>26)</sup>. Theoretical estimates from different groups are reported; the last (red) point includes the KLOE new measurement. Right: Pion form factor measured by KLOE, compared with CMD-2, SND.*

### 3.2 The measurement of the branching ratio and the search for a CP violating asymmetry in the $\eta \rightarrow \pi^+\pi^-e^+e^-$ decay

There are several theoretical reasons to study the  $\eta \rightarrow \pi^+\pi^-e^+e^-$  decay. It allows to probe the structure of the  $\eta$  meson <sup>28)</sup>, to compare the predictions of the branching ratio value based on Vector Meson Dominance model, and ChPT <sup>29, 30, 31, 32)</sup> and to study CP violation beyond the prediction of the Standard Model <sup>33)</sup> measuring the angular asymmetry between pions and electrons decay planes.

The samples used in this analysis are: 1733 pb<sup>-1</sup> from 2004-2005 data taking; 232 pb<sup>-1</sup> from 2006 off-peak ( $\sqrt{s} = 1000$  MeV) data taking; Montecarlo signal and background equivalent to  $50 \times 10^3$  pb<sup>-1</sup> and 3447 pb<sup>-1</sup>, respectively. The signal MC has been produced using the PHOTOS package to account for FSR.

The events are required to have at least four tracks (two positive and two negative) coming from a cylinder around the Interaction Point (radius  $R = 4$  cm, height  $h = 20$  cm). For each charge, the two tracks with the highest momenta are selected. A cluster not associated to any track, having time compatible with the photon time of flight, energy of at least 250 MeV and in the polar-angle range ( $23^\circ - 157^\circ$ ), is also required.

Background sources can be grouped into  $\phi$ -decays and events in the continuum. The former is mainly due to  $\phi \rightarrow \pi^+\pi^-\pi^0$  events (with  $\pi^0$  Dalitz decay) and to  $\phi \rightarrow \eta\gamma$  events either with  $\eta \rightarrow \pi^+\pi^-\pi^0$  (with  $\pi^0$  Dalitz decay) or with  $\eta \rightarrow \pi^+\pi^-\gamma$  (with photon conversion on the beam pipe). The latter is due to  $e^+e^- \rightarrow e^+e^-(\gamma)$  events with photon conversions, split tracks or interactions with some material in the region of DAΦNE quadrupoles inside KLOE. Because of poor MC statistics, this background has been studied using off-peak data taken at  $\sqrt{s} = 1$  GeV, where  $\phi$  decays are negligible. Backgrounds are rejected applying cuts on: 1- the momenta ( $(270 < |\vec{p}(p_{Max}^+)| + |\vec{p}(p_{Max}^-)| < 460)$  MeV and  $(450 < \sum_1^4 |\vec{p}_i| < 600)$  MeV); 2- the invariant mass

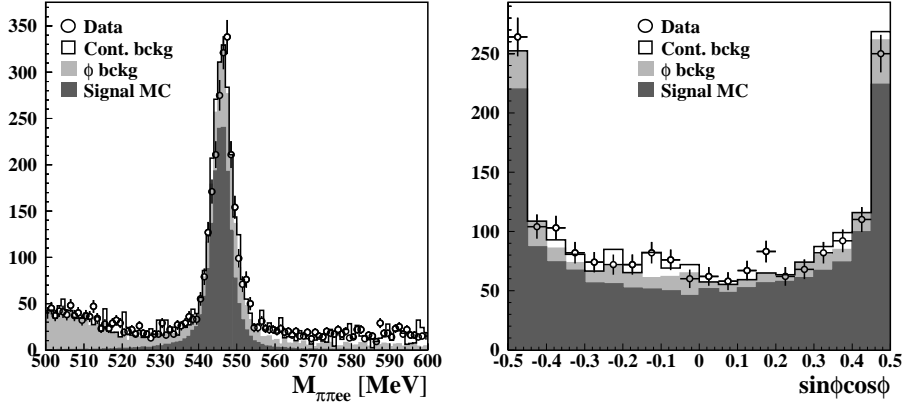


Figure 7: *Left: fit to the invariant mass of the four selected tracks. Right: distribution of the  $\sin\phi\cos\phi$  variable in the signal region. Dots: data. The black histogram is the expected distribution, i.e. signal MC (dark grey),  $\phi$  background (light grey) and background in the continuum (white).*

and the distance of the candidate electron tracks to reject photon conversions on the beam pipe ( $M_{ee}(BP) < 15$  MeVs and  $D_{ee}(BP) < 2.5$  cm); 3- the average polar angle of forward and backward particles identified as signal to reject background in the continuum ( $\langle \cos\theta_f \rangle > 0.85$  and  $\langle \cos\theta_b \rangle < -0.85$ ).

Background contribution is evaluated performing a fit to the data distribution of the  $\pi^+\pi^-e^+e^-$  invariant mass after the cuts on the momenta using as input background shapes only. The fit is done on sidebands in order not to introduce correlations between signal and background ( $[450, 520]$  MeV  $\cup$   $[570, 650]$  MeV). The output of the fit ( $\chi^2/dof = 32.5/30$ ,  $P(\chi^2) = 0.35$ ) is shown in the left panel of Fig. 7. For the signal estimate we limit ourselves to the region  $[535, 555]$  MeV and perform the event counting after background subtraction: we find 1555 (368) signal (background) events. The selection efficiency has been evaluated from MC.

The result obtained for the branching ratio is:

$$BR(\eta \rightarrow \pi^+\pi^-e^+e^-\gamma) = (26.8 \pm 0.9_{Stat.} \pm 0.7_{Syst.}) \times 10^{-5}. \quad (13)$$

The decay plane asymmetry is calculated starting from the momenta of the four particles and is expressed as function of the angle  $\phi$  between the pion and the electron planes in the  $\eta$  rest frame. It has been evaluated for the events in the signal region after background subtraction. The value obtained is:

$$\mathcal{A}_\phi = (-0.6 \pm 2.5_{Stat.} \pm 1.8_{Syst.}) \times 10^{-2} \quad (14)$$

which is the first measurement of this asymmetry. The distribution of the  $\sin\phi\cos\phi$  variable is shown in the right panel of Fig. 7.

The results are final and a paper has been submitted to PLB. The same four track final state is also under study to select the  $\eta \rightarrow e^+e^-e^+e^-$ , never observed before.

### 3.3 Radiative decay of eta meson, $\eta \rightarrow \pi^+\pi^-\gamma$

In the  $\eta \rightarrow \pi^+\pi^-\gamma$  decay a significant contribution from chiral anomaly responsible for  $\eta \rightarrow \gamma\gamma$  decay is expected<sup>34)</sup>. Chiral anomaly describes the non-resonant coupling providing the distribution of the invariant mass of the pions ( $m_{\pi\pi}$ ). The measurement of  $m_{\pi\pi}$  is relevant to disentangle resonant contributions, e.g. from the  $\rho$ -meson. Several theoretical approaches have been developed to treat the contribution of the anomalies to the decay<sup>35) 36) 37)</sup>. This decay has been measured in the 1970s with data samples of the order of  $10^4$  events<sup>38) 39)</sup>. However, the theoretical papers which tried to combine the measurements found discrepancies in data treatment and problems with obtaining consistent results. Therefore, the results from experiments with large statistics are really needed to clarify the situation<sup>40)</sup>.

KLOE data contains about  $3.5 \times 10^6$   $\eta \rightarrow \pi^+\pi^-\gamma$  decays. With this statistics it is possible to investigate in detail the pion invariant mass distribution and the photon energy spectrum in order to disentangle non-resonant contributions and settle the inconsistencies of previous measurements. The measurement of the branching ratio of the  $\eta \rightarrow \pi^+\pi^-\gamma$  decay will have an impact on the analysis of the rare  $\eta$  decays like  $\eta \rightarrow \pi^+\pi^-e^+e^-$  and  $\eta \rightarrow \pi^+\pi^-\mu^+\mu^-$  and, last but not least, the decay gives the opportunity to search for C violation signature in the left-right charge asymmetry.

The main background is the  $\phi$  decay  $\phi \rightarrow \pi^+\pi^-\pi^0$  (with ratio 200:1 to our signal) which mimics the event signature in the specific kinematical range when two photons (one coming from eta,  $\gamma_\eta$ , and the other,  $\gamma_\phi$ , from  $\phi$  decay) invariant mass is in the range of the  $\pi^0$  reconstructed mass. In order to reduce background contribution, the following steps are made:

1. At least 2 neutral clusters<sup>1</sup> must be found and at least one of them with energy  $> 250$  MeV (photon with maximum energy is assumed to originate from  $\phi \rightarrow \eta\gamma$  decay). Two tracks (one positive and one negative) are selected on the basis of the distance of closest approach to the interaction point.
2. We improve the energy resolution on  $\gamma_\phi$  using the constraints from the two-body kinematics of  $\phi \rightarrow \eta\gamma$  decay, allowing to calculate photon energy from angular information only. Then, using event kinematics from  $\phi \rightarrow \gamma\eta(\rightarrow \pi^+\pi^-\gamma)$  decay chain (with improved information about  $\gamma_\phi$ ) we calculate the  $\gamma_\eta$  momentum and use the opening angle ( $\alpha$ ) between this vector and the measured direction of each neutral cluster (if there are more than one) in order to select the cluster with minimum  $\alpha$  as originating from the  $\eta \rightarrow \pi^+\pi^-\gamma$  decay. Thereafter we require that selected  $\gamma_\eta$  has:  $|E_\gamma - P_\gamma| < 10$  MeV and  $\alpha < 0.2$  rad.

The selection efficiency for the signal and background contributions after each step is summarized in Table 1. The selection criteria allow to retain 50% of the signal while reducing signal-to-background ratio to 1:8. The efficiency distribution as a function of the energy of  $\gamma_\eta$  (fig.8, left) has a smooth behaviour in most of the kinematical range. The same figure (picture on the right-hand side) shows the distribution of the cosine of the angle  $\beta$  between  $\gamma_\phi$  and  $\gamma_\eta$ , calculated in the  $\pi^0$  rest frame, as the photons were coming from  $\pi^0$  decay (background hypothesis). Background (mostly events from  $\phi \rightarrow \pi^+\pi^-\pi^0$  decay) peaks strongly at  $\cos\beta = -1$  while the signal is

---

<sup>1</sup>A cluster is defined neutral if it does not have any associated track and has a time compatible with the photon time of flight.

more uniformly distributed. Summing MC-predicted contributions from signal and background we obtain a very good agreement with the experimental data, so that cuts on the  $\cos\beta$  distribution can be well controlled by our simulation, allowing further background reduction with small systematic uncertainty. Studies are underway to finalize the selection procedure.

Table 1: Selection efficiency for signal and background of the part of the analysis procedure described in the text.

	Event signature		Pre-selection	
	efficiency	signal-to-bkg ratio	efficiency	signal-to-bkg ratio
SIGNAL	58%	1 : 100	50%	1 : 8
BACKGROUND	53%		3.5%	

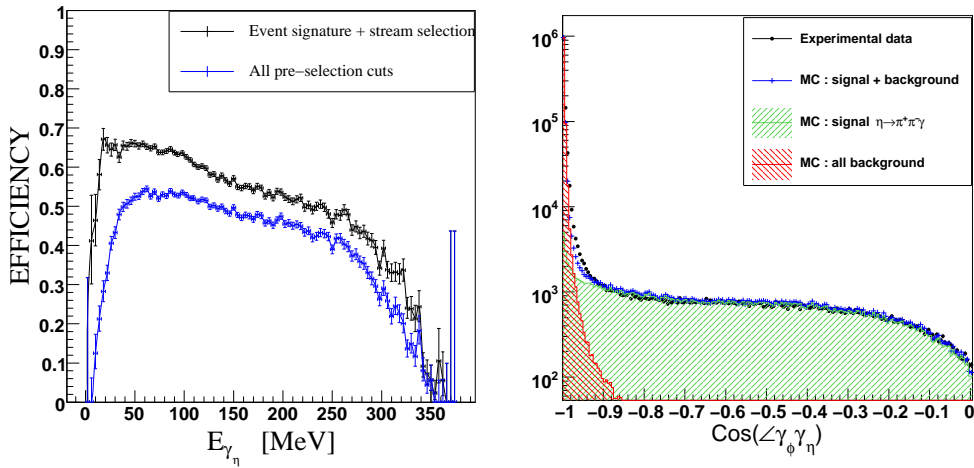


Figure 8: The efficiency distribution as function of the energy of  $\gamma_\eta$  (left). Distribution of the cosine of the angle between  $\gamma_\phi$  and  $\gamma_\eta$  calculated in the rest frame of  $\pi^0$  (background hypothesis) (right).

## 4 KLOE2

### 4.1 Studies for the $\gamma\gamma$ tagger

$\gamma\gamma$  physics <sup>41)</sup> at the  $e^+e^-$  colliders gives access to states with  $J^{PC} = 0^{\pm\pm}, 2^{\pm\pm}$ , not directly coupled to the photon ( $J^{PC} = 1^{--}$ ).

The cross section  $\sigma(\gamma\gamma \rightarrow X)$  was studied at PETRA, CESR, LEP and at the B-factories over the years. In the low-energy region,  $m_\pi \leq W_{\gamma\gamma} \leq 700$  MeV, measurements <sup>42)</sup> are affected by large statistical and systematic uncertainties due to small detection efficiencies, large background contributions and particle identification ambiguities in the low-mass hadronic systems.

KLOE2 is the ideal place for precision measurements of low-mass hadronic systems with high statistics and well controlled systematic errors.

Many interesting channels can be investigated and both, the two-photon width of light pseudoscalar mesons, and the meson transition form factors <sup>43)</sup> can be obtained. Search for  $\sigma$  meson is another interesting topic addressed by the  $\gamma\gamma$  physics program.

The  $\sigma$  meson was suggested for the first time by the linear sigma model, describing pion-nucleon interaction. For many years, the experimental studies did not find any clear signal of this meson, whose existence and nature (i.e. quark substructure) remained controversial.

The situation has only recently changed. It has been shown <sup>44)</sup> that the  $\pi\pi$  scattering amplitude contains a pole with the quantum numbers of vacuum, a mass  $M_\sigma = 441^{+16}_-8$  MeV and a width  $\Gamma_\sigma = 544^{+25}_{-18}$  MeV. The  $\sigma$  has been looked for also in  $D$  decays by the E791 Collaboration at Fermilab <sup>45)</sup>. From the  $D \rightarrow 3\pi$  Dalitz plot analysis, E791 finds that almost 46% of the width is due to  $D \rightarrow \sigma\pi$  with a  $M_\sigma = 478 \pm 23 \pm 17$  MeV and  $\Gamma_\sigma = 324 \pm 40 \pm 21$  MeV. BES <sup>46)</sup> has looked for  $\sigma$  in  $J/\psi \rightarrow \omega\pi^+\pi^-$ , obtaining a mass value of  $M_\sigma = 541 \pm 39$  MeV and a width of  $\Gamma_\sigma = 252 \pm 42$  MeV.

It is worth to notice that the problem of assessing the existence and nature of the  $\sigma$  meson is not confined to low energy phenomenology. Just to mention a possible relevant physical scenario in which  $\sigma$  could play a role, consider the contamination of  $B \rightarrow \sigma\pi$  in  $B \rightarrow \rho\pi$  decays (possible because of the large  $\sigma$  width). This could sensibly affect the isospin analysis for the CKM- $\alpha$  angle extraction <sup>47)</sup>. Similarly, recent studies of the  $\gamma$  angle through a Dalitz analysis of neutral  $D$  decays call for the  $\sigma$  resonance to fit data <sup>48)</sup>.

The only available data at low energy come from Crystal Ball <sup>42)</sup> and JADE <sup>49)</sup> collaborations. Their precision does not allow to reach any firm conclusion on the presence of a resonance in the region of (400-500) MeV. KLOE2 data are very much awaited to clarify the situation.

To improve on the measurement of the  $\gamma\gamma \rightarrow \pi\pi$  cross section, high statistics has to be complemented by a careful control of the systematics which cannot be obtained without strong reduction of background events.

The main source of background comes from  $\phi$  decays. Studies currently underway on the KLOE data sample are using the off-peak data in order to evaluate the experimental capabilities leaving aside most of the background from  $\phi$  decays. At KLOE2 we aim to analyze the on-peak sample performing background suppression with the information coming from a tagger system for efficient detection of scattered electrons.

Scattered electrons from  $\gamma\gamma$  reaction deviate from the main orbit while propagating on the machine lattice. For the design of the tagging system we have performed MonteCarlo studies of the trajectories of scattered electrons, whose initial kinematical distribution is given by purpose-made  $\gamma\gamma$  generators. The magnetic layout of DAΦNE has been fully treated.

The results show that the constraints coming from the DAΦNE structure do not prevent KLOE2 from obtaining a good coverage of the kinematic region of interest.

Satisfactory results have been shown using a tagger system composed by two stations located at  $\sim 1$  m and  $\sim 11$  m from the IP:

- a station to detect leptons at low energy (LET), located in the region between the two quadrupoles inside KLOE (QD0 and QF1). According to the tracking, the energy of the

scattered leptons arriving on this detector is mostly in the interval (160-230) MeV;

- a station for leptons with high energy (HET), located at the exit of the first bending magnet (about 11 m from the IP). The energy of the scattered particles is in this case mostly in the range (425-490) MeV. The upper limit of the interval is determined by the minimum distance (3 cm) from the main orbit where we can place the detector without interfere with proper DAΦNE operations.

Scattered leptons on the LET detector pass through the first quadrupole, QD0 and, being off-energy, are deflected with respect to the main orbit. Energy distribution of these leptons is very broad, with tails reaching 50 MeV on one side and 450 MeV on the other. The measurement of the lepton energy requires a calorimeter, being the position of the exit point slightly correlated with the lepton momentum.

The HET detectors are located 11 m from the IP. The leptons propagate through the magnetic layout of the machine, and are selected by the B-fields according to their momenta. Only leptons within a cone of  $\Delta\theta < 40$  mrad, with the axis on the flight direction of the incoming beam, are detected. A position detector in this case can measure the lepton momentum with good precision (fig.9).

A detector 7 cm long can tag leptons with energy between 430 and 475 MeV.

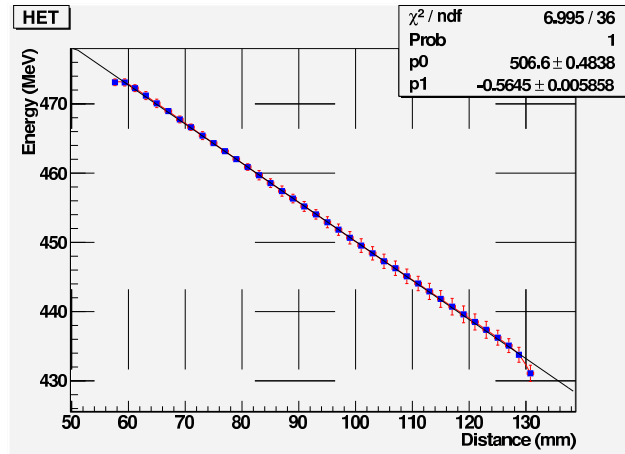


Figure 9: *Energy of the leptons on the HET as a function of the displacement from main orbit.*

When both scattered leptons are detected in the HET/LET taggers we can measure, independently from KLOE, the two-photon centre-of-mass energy  $W_{\gamma\gamma}$  of the reaction  $\gamma\gamma \rightarrow \pi^0\pi^0$ .

With the realistic assumption of a 2 mm pitch for the HET and a LET resolution of  $\sigma(E)/E = 5\%/\sqrt{E(\text{GeV})}$ , in case of coincidence HET  $\otimes$  LET we obtain a resolution on  $W_{\gamma\gamma}$  of  $\sigma_E = 12.8$  MeV, while in the case of coincidence LET  $\otimes$  LET the resolution is  $\sigma_E = 33.4$  MeV.

On this basis, the design of the tagger detectors is being prepared. Tests for the choice of the crystals and the readout electronics have been carried out at the Frascati beam test facility. The Technical Design Report will be submitted for approval to the INFN by the end of March, 2009.

## 4.2 Studies for quadrupole instrumentation and calorimeters at low polar angle

The new DAΦNE interaction region, adopting the crab-waist scheme, has the two beam pipes already separated at  $\sim 55$  cm from the IP, well inside the KLOE detector, and before the focusing quadrupoles QF1 (fig.10). For this reason the old instrumentation of the quadrupole zone, needed to veto photons from Kaon decay in the drift chamber, has to be replaced.

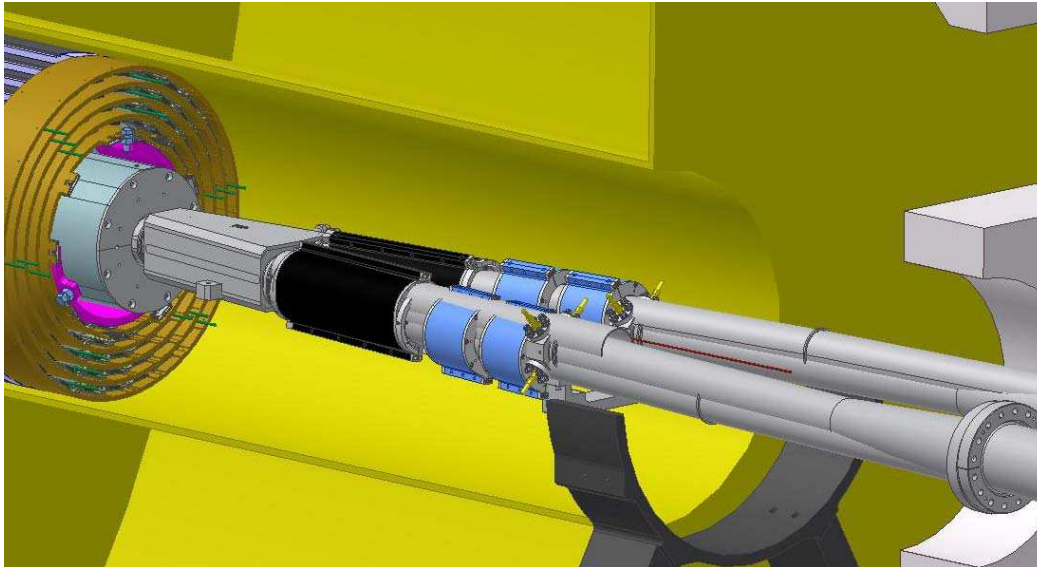


Figure 10: *DAΦNE beam pipe inside KLOE.*

The project, QCALT, requires the realization of a calorimeter composed by  $12 + 12$  modules of tungsten and scintillating tiles coupled with optical fibers for signal transmission to the Silicon-PhotoMultipliers. Each module,  $\sim 90$  cm long, is longitudinally divided into 18 tiles, and radially into 5 planes interspaced with tungsten, for a total of 5.7 radiation lengths (the maximum possible absorber in the available space). Electronics for power supply and readout cards, that are custom boards with pre-amplifier, HV distributor and controller, are being designed and realized by the LNF Electronics Service. The study of the tile-fiber and fiber-SiPM couplings is well advanced, as well as the design of the mechanical structure of the detector and its integration on the DAΦNE / KLOE central region.

We plan to realize an entire calorimeter module by the end of year 2009 to finalize the construction procedure and to measure at the LNF test beam the calorimeter performance with electrons of energy up to 500 MeV.

The group is also working on the R&D for a crystal (LYSO) calorimeter, CCALT, to detect low polar angle photons from the interaction region. An integrated plan to test the crystals for CCALT and for the LET station of the  $\gamma\gamma$  tagger, is being followed. Test beams are being realized to study both, the crystal performance, and the response of the custom readout electronics.

### 4.3 R&D for the KLOE2 inner tracker

A fully cylindrical and dead-zone-free GEM detector has been designed as inner tracker for the upgrade of the KLOE detector. The proposed inner tracker, that opens the way for a new and competitive category of ultra-light, full sensitive vertex detectors for high energy physics experiments, will play a crucial role in the study of the  $K_S$  and  $\eta$  rare decays and in the measurement of the neutral kaon interferometry. Main requirements are: good spatial resolution,  $\sigma(r\phi) = 200 \mu m$  and  $\sigma(z) = 500 \mu m$  and very low material budget, 2% of  $X_0$  for the whole detector. The inner tracker will be composed by five layers of cylindrical triple-GEM detectors (CGEM), covering the space from the beam pipe to the inner wall of the KLOE Drift Chamber (from 150 mm to 250 mm radius). Each CGEM is realized inserting one into the other five cylinders made of thin ( $50 \mu m$ ) polyimide foils: the cathode, the three GEMs and the anode readout. In order to avoid support frames inside the sensitive volume, the cylindrical GEMs are mechanically stretched from their ends where annular fiberglass frames are glued. The final result is a very light detector: only 0.2% of  $X_0$  per layer inside the active area. The readout will be performed with a XV pattern of readout strips engraved on the anode foil<sup>50</sup>). A full scale prototype (300 mm diameter, 360 mm length) of the first layer of the inner tracker has been successfully built and characterized under different experimental conditions. The results show that this technology can be successfully used for tracking improvement at KLOE2. A description of the construction procedure and the detector performance is given in the following section.

#### 4.3.1 The CGEM prototype

In 2007 a CGEM prototype has been built with the same diameter of the innermost IT layer (300 mm) and a reduced length of 360 mm. For sake of simplicity the anode has been segmented only with longitudinal strips, with a pitch of  $650 \mu m$ , providing the  $r\phi$  coordinate. About 320 strips out of 1500 have been connected to FEE and readout.

Each CGEM is a Triple-GEM detector with a geometrical configuration of the gaps of 3/2/2/2 mm, respectively for drift/transfer1/transfer2/induction. The cathode is internal to the anode.

Three GEM foils are glued together at first, to obtain the single large foil needed to make a cylindrical electrode. We used an epoxy glue (Araldite), distributed along one edge of the GEM, on a 3 mm wide region. Then foil is rolled on an aluminum mould coated with a precision machined Teflon film providing a non-stick, low friction surface. The mould is then enveloped in a vacuum bag and vacuum is applied with a Venturi system, resulting in a uniform pressure of  $0.8 \text{ Kg/cm}^2$  throughout the whole surface. At this step two fiberglass annular rings are also glued at the edges of the electrode, representing all the mechanical frames needed to support the detector. After the curing cycle of the glue the cylindrical electrode is extracted from the mould. Cathode and anode are obtained with the same procedure. At the end the five electrodes are inserted one into the other and the detector is sealed with epoxy on both sides<sup>51</sup>).

The mechanical tension needed by the GEM foil in order to avoid oscillation and instability is given by hanging the prototype and applying a traction along its axis. A detailed simulation has been performed with the ANSYS program in order to evaluate the static and dynamic behavior of the detector. In particular, we found that for a 100 N longitudinal traction the elongation is about

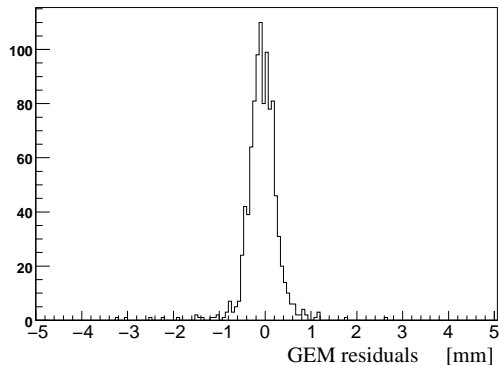


Figure 11: *Distribution of tracking residuals showing  $\sigma_{res} = 250 \mu\text{m}$ .*

0.03 mm, and the sagitta due the gravity is only  $6 \mu\text{m}$ . We have experimentally verified that such a traction is enough to obtain a proper operation of the chamber.

The final IT detector will require GEM foils with an active area as large as  $700 \times 500 \text{ cm}^2$ . The ST-DEM-PMT laboratory at CERN, where GEMs are produced, is planning a change of technology in order to realize such large area foils, leading to a different shape of the holes. We are both simulating the new GEM and building small prototypes in order to determine the operation parameters, such as gain, electron transparencies, charging-up, ion feedback.

The C-GEM prototype has first been tested in current mode with a 6 keV X-ray gun. A  $10 \times 10 \text{ cm}^2$  planar GEM has been placed in the same gas line and used as a reference in order to normalize the gain for changes of atmospheric variables. The gas gain has been measured up to a value of  $2 \times 10^4$  and no discharge has been observed. The electron transparency has been measured as a function of the electric field, obtaining results in good agreement with expectations. Gain fluctuations throughout the 940 mm of circumference were within 9%, showing good uniformity on such a large surface.

Then, the prototype has been extensively tested with the 10 GeV pion beam at the T9 area of CERN PS. Here 128 channels have been equipped with the new GASTONE ASIC, which has been developed for the KLOE2 experiment, in order to fulfill low-power consumption and high integration requirements. It is composed of four different blocks: a charge sensitive preamplifier (20 mV/fC sensitivity), a shaper, a leading edge discriminator and a monostable circuit to stretch the digital signal waiting for the KLOE L1 trigger. While a version with 64 channels has been designed for the final readout card<sup>52)</sup>, we mounted on the detector the first release of the ASIC, with 16 channels.

The detector was flushed with a  $\text{Ar}/\text{CO}_2 = 70/30$  gas mixture and operated at a gain of  $2 \times 10^4$ . Figure 11 shows the residuals of the clusters with respect to the reconstructed position of the track. The spatial resolution of the external tracker was  $\sigma_{trk} = 140 \mu\text{m}$ . Subtracting this contribution, the GEM spatial resolution is:

$$\sigma_{GEM} = \sqrt{\sigma_{res}^2 - \sigma_{trk}^2} \simeq 200 \mu\text{m} \quad (15)$$

in agreement with expectations from a digital readout of  $650 \mu\text{m}$  pitch strips.

The efficiency of the chamber has been measured for different track positions. In most of the region a very high efficiency of 99.6% has been obtained. Time distributions in normal regions of the chamber and in the junction zones of the foils have been studied. In the normal region a 13 ns RMS is obtained, in agreement with the performance of the gas mixture. In the gluing zone, representing less than 0.4% of the surface, the spectrum is much broader, with a 200 ns RMS. In particular, the signals are delayed up to 700 ns, suggesting a longer drift path to reach the anode. Such hypothesis has been confirmed by simulations with ANSYS and GARFIELD, showing a distortion of the field lines in the gluing regions due to space charge on the dielectric.

## 5 KLOE papers in year 2008

1. F. Ambrosino *et al.*, *J. High Energy Phys.* **02**, 09 (2008).
2. F. Ambrosino *et al.*, *J. High Energy Phys.* **01**, 073 (2008).
3. F. Ambrosino *et al.*, *J. High Energy Phys.* **0804**, 059 (2008).
4. F. Ambrosino *et al.*, *J. High Energy Phys.* **0805**, 006 (2008).
5. F. Ambrosino *et al.*, *J. High Energy Phys.* **0805**, 051 (2008).
6. F. Ambrosino *et al.*, *Eur. Phys. J. C* **55**, 539 (2008).
7. F. Ambrosino *et al.*, *Phys. Lett. B* **666**, 305 (2008).
8. F. Ambrosino *et al.*, *Phys. Lett. B* **669**, 223 (2008).
9. F. Bossi *et al.*, *Riv. Nuovo Cim.* **031**, 531 (2008).

## 6 Public notes in year 2008

1. A. De Santis and S. Giovannella, “Study of the  $e^+e^- \rightarrow \omega\pi^0 \rightarrow \pi^+\pi^-\pi^0\pi^0$  process using KLOE data”, KLOE Note 219, July 2008.
2. A. De Santis, S. Giovannella, and S. Miscetti, “Updates of the measurement of the  $e^+e^- \rightarrow \omega\pi^0 \rightarrow \pi^0\pi^0\gamma$  cross section using 2001-2006 KLOE data”, KLOE Note 220, July 2008.
3. S. Müller *et al.*, “Measurement of  $\sigma(\pi^+\pi^-\gamma)$  using initial state radiation and extraction of  $\Delta a_\mu^{\pi\pi}$  for  $[0.35,0.95]$  GeV<sup>2</sup> with the KLOE experiment”, KLOE Note 221, September 2008.

## 7 Contributions to Conferences and Seminars

1. C. Gatti, “K decays measurements with the KLOE detector”, Les Rencontres de Physique de la Vallée d’Aoste, La Thuile, Italy, 24 Feb-1 Mar, 2008.
2. M. Testa, “Recent results from KLOE”, 43rd Rencontres de Moriond on Electroweak Interactions and Unified Theories, La Thuile, Italy, Mar 1-8, 2008.

3. F. Nguyen , “A precise new KLOE measurement of  $F(\pi)$  with ISR events and determination of  $\pi\pi$  contribution to  $a_\mu$  for  $[0.35,0.95]$   $\text{GeV}^2$ ”, PhiPSI08, Frascati, Italy, 7-10 Apr, 2008.
4. T. Spadaro, “ $K_{e2}$  measurements and lepton flavor universality”, Heavy Quarks and Leptons, Melbourne, Australia, June 5-9, 2008.
5. T. Capussela, “ $\eta \rightarrow \pi\pi\pi$  Dalitz plot analysis”, FlaviaNet Workshop, Anacapri, June 12-14, 2008.
6. E. De Lucia, “Results on  $V_{us}$ ”, FlaviaNet Workshop, Anacapri, June 12-14, 2008.
7. M. Martini, “ $K_S \rightarrow \gamma\gamma$  and  $Ke3\gamma$  decays”, FlaviaNet Workshop, Anacapri, June 12-14, 2008.
8. R. Versaci, “KLOE study on  $\eta \rightarrow \pi\pi e e$ ”, FlaviaNet Workshop, Anacapri, June 12-14, 2008.
9. M. Palutan, “CPT test from unitarity”, FlaviaNet Workshop, Anacapri, June 12-14, 2008.
10. T. Spadaro, “Precision test of the SM with leptonic and semileptonic kaon decays at KLOE”, BEACH 2008, University of South Carolina, Columbia, June 22-28, 2008.
11. M. Antonelli, “ $V_{us}$  and lepton universality from K decays with the KLOE detector”, PIC 2008, Perugia, Italy, June 25-28, 2008.
12. S. Mueller, “KLOE results on  $e^+e^-$  hadronic cross section”, QCD 2008, Montpellier, France, July 7-12, 2008.
13. M. Palutan, “Measurement of  $V_{us}$  from kaon decays with KLOE”, Meeting del Comitato di Valutazione Internazionale dell’INFN, Roma, July 9, 2008.
14. E. De Lucia , “Unitarity and universality with kaon physics at KLOE”, ICHEP 2008, Philadelphia, Pennsylvania, 30 Jul - 5 Aug, 2008.
15. B. Sciascia , “ $K_{e2}^\pm$  search and lepton flavor violation at KLOE”, ICHEP 2008, Philadelphia, Pennsylvania, 30 Jul - 5 Aug, 2008.
16. T. Capussela, “Results from the KLOE collaboration: study of  $\eta/\eta'$  meson”, Confinement 08, Mainz, Germany, Sep 1-6, 2008.
17. A. Sibidanov, “Measurements of  $V_{us}$  from Kaon decays at KLOE”, CKM 08, Rome, Italy, Sep 9-13, 2008.
18. T. Spadaro, “ $K_{l2}$  Review”, CKM 0, Rome, Italy, Sep 9-13, 2008.
19. V. Patera, “Future Experiments at DAFNE, the Frascati  $\phi$  factory”, PANIC 08, Eilat, Israel, Nov 9-14, 2008.
20. F. Bossi, “The KLOE2 project”, Discrete 08, Valencia, Spain, Dec 11-16, 2008.
21. R. Versaci, “Study of  $\eta \rightarrow \pi\pi e e$  at KLOE”, Discrete 08, Valencia, Spain, Dec 11-16, 2008.

## References

1. A. Masiero, P. Paradisi, and R. Petronzio, Phys. Rev. D **74**, 011701 (2006).
2. F. Ambrosino *et al.* [KLOE Coll.], Phys. Lett. B **636**, 173 (2006).
3. F. Ambrosino *et al.* [KLOE Coll.], Phys. Lett. B **632**, 43 (2006).
4. F. Ambrosino *et al.* [KLOE Coll.], J. High Energy Phys. **02**, 098 (2008).
5. F. Ambrosino *et al.* [KLOE Coll.], Phys. Lett. B **666**, 305 (2008).
6. F. Ambrosino *et al.* [KLOE Coll.], Phys. Lett. B **632**, 76 (2006).
7. F. Ambrosino *et al.* [KLOE Coll.], Phys. Lett. B **626**, 15 (2005).
8. F. Ambrosino *et al.* [KLOE Coll.], Phys. Lett. B **636**, 166 (2006).
9. F. Ambrosino *et al.* [KLOE Coll.], J. High Energy Phys. **12**, 105 (2007).
10. W. M. Yao *et al.*, J. Phys. G **33**, 1 (2006).
11. P.A. Boyle *et al.* [RBC/UKQCD Coll.], arXiv:0710.5136.
12. W. Marciano, Phys. Rev. Lett. **93**, 231803 (2004).
13. E. Follana *et al.* [HPQCD/UKQCD Coll.], arXiv:0706.1726.
14. I.S. Towner and J.C. Hardy, arXiv:0710.3181.
15. F. Ambrosino *et al.* [KLOE Coll.], Phys. Lett. B **642**, 315 (2006).
16. J. Bernabeu, N. Mavromatos, J. Papavassiliou, Phys. Rev. Lett. **92**, 131601 (2004).
17. J. Bernabeu *et al.*, Nucl. Phys. B **744**, 180 (2006).
18. G. Ecker and A. Pich, Nucl. Phys. B **366**, 189 (1991).
19. A. Angelopoulos *et al.* [CLEAN Coll.], Phys. Lett. **B**, 413 (1997) 232.
20. F. Ambrosino *et al.* [KLOE Coll.], Phys. Lett. B **672**, 203 (2009).
21. I.H. Chiang *et al.*, Phys. Rev. D **6**, 1254 (1972).
22. F. Ambrosino *et al.*, [KLOE Coll.] Phys. Lett. B **670**, 285 (2009).
23. A. Aloisio *et al.*, [KLOE Coll.] Phys. Lett. B **606**, 12 (2005).
24. R. R. Akhmetshin *et al.* [CMD-2 Coll.], Phys. Lett. B **648**, 28 (2007);  
M. N. Achasov *et al.* [SND Coll.], J. Exp. Theor. Phys. **103**, 380 (2006).
25. F. Jegerlehner and A. Nyffeler, arXiv:0902.3360.

26. G. W. Bennett *et al.* [Muon g-2 Coll.], Phys. Rev. Lett. **89**, 101804 (2002); Erratum *ibid.*, **89**, 129903 (2002).
27. Proc. of PhiPsi08 Conference, Frascati, Italy, 7-10 April 2008, Eds. C. Bini and G. Venanzoni, Nucl. Phys. B Proc. Suppl. **181-182**.
28. L. G. Landsberg, Phys. Rept. **128**, 301 (1985).
29. C. Jarlskog and H. Pilkuhn, Nucl. Phys. B **1**, 264 (1967).
30. A. Faessler, C. Fuchs, and M. I. Krivoruchenko, Phys. Rev. C **61**, 035206 (2000) .
31. C. Picciotto and S. Richardson, Phys. Rev. D **48**, 3395 (1993).
32. B. Borasoy and R. Nissler, arXiv:0705.0954.
33. D. N. Gao, Mod. Phys. Lett. A **17**, 1583 (2002).
34. S.L. Adler, Phys. Rev. **177**, 2426 (1969).
35. B.R. Holstein, Phys. Scripta T **99**, 55 (2002).
36. M. Benayoun *et al.*, Eur. Phys. J. C **31**, 525 (2003).
37. B. Borasoy and R. Nissler, Nucl. Phys. A **740**, 362 (2004).
38. P. Gormley, Phys. Rev. D **2** (1970) 501.
39. J. Layter, Phys. Rev. D **7**, 2565 (1973).
40. B. Borasoy and R. Nissler, arXiv:0705.0954.
41. see the review by M. R. Pennington, arXiv:hep-ph/0511146, and reference therein.
42. H. Marsiske *et al.* (Crystal Ball Collab.), Phys. Rev. D **41**, 3324 (1990).
43. F. Ambrosino *et al.*, Eur. Phys. J. C **50**, 729 (2007).
44. I. Caprini, G. Colangelo and H. Leutwyler, Phys. Rev. Lett. **96**, 132001 (2006).
45. E.M. Aitala *et al.*, [E791 Coll.], Phys. Rev. Lett. **86**, 770 (2001).
46. M. Ablikim *et al.*, [BES Coll.], Phys. Lett. B **598**, 149 (2004).
47. A. Deandrea and A.D. Polosa, Phys. Rev. Lett. **86**, 216 (2001); S. Gardner and U. Meissner, Phys. Rev. D **65**, 094004 (2002); I. Bigi, arXiv:hep-ph/0601167.
48. B. Aubert *et al.*, [BaBar Coll.], Phys. Rev. Lett. **95**, 121802 (2005).
49. T. Oest *et al.*, [JADE Coll.], Z. Phys. C **47**, 343 (1990).
50. D. Domenici, Frascati Physics Series Vol. XLVI (2007) pp. 1477-1484.
51. G. Bencivenni *et al.*, NSS Conference Record, IEEE Volume **6**, 4666-4670 (2007).
52. A. Balla *et al.*, in 8<sup>th</sup> International Conference on Position Sensitive Detectors. 1-5 September 2008, Glasgow (UK).